Journal of Molecular Catalysis A: Chemical 356 (2012) 106–113

Contents lists available at SciVerse ScienceDirect

Journal of Molecular Catalysis A: Chemical

journal homepage: www.elsevier.com/locate/molcata

Silver (I) activated quaternization of tertiary amines by alkyl iodides: Overall analysis coupling homogeneous and heterogeneous processes

M. Soledade C.S. Santos, Ester F.G. Barbosa*

Centro de Química e Bioquímica, DQB, Faculdade de Ciências, Universidade de Lisboa, 1749-016 Lisboa, Portugal

ARTICLE INFO

Article history:
Received 21 October 2011
Accepted 31 December 2011
Available online 10 January 2012

Keywords:
Homogeneous and heterogeneous catalysis
Silver (I) activated amine quaternization
Interfacial molecular thickness
Linking bidimensional and tridimensional workspaces

ABSTRACT

Kinetic data for the silver (I) activated homogeneous and heterogeneous quaternization of tributylamine by alkyl iodides in toluene is presented. Silver iodide was used as a solid catalyst. Solution and surface parameters were obtained applying the multistep kinetic model, previously proposed by Santos and Barbosa. A scrutiny of the derived quantities evidences competing structural and electronic effects. The solution reaction is dominated by structural factors while electronic effects govern the surface process. An overall analysis considering data from triethylamine systems, earlier investigated, allowed the establishment of a parallelism between the homogeneous and heterogeneous processes. A molecular level study involving size, shape and orientation of the chemical species on the surface, lead to estimates of interfacial layer thicknesses. A combination of surface parameters superficial reacting monolayer thicknesses and, the parallelism between homogeneous and heterogeneous catalysis consented the evaluation of "volumetric surface rate constants" which are directly comparable with their solution counterparts.

1. Introduction

Weak intermolecular forces dictate how and why molecules fit together, commanding binding, solubilization, reaction pathways, stereochemistry and molecular recognition phenomena. Over the last forty years, considerable efforts have been made, aiming a molecular understanding of chemical and biochemical processes such as homogeneous, heterogeneous and biological catalysis. Major progresses in surface and colloid chemistry were of utmost importance, making relevant contributions to the development of experimental, simulation and theoretical methods. Several approaches, seeking specific localization and alignment of molecules, imparted by surfaces or media confinements, have been attempted [1–7]. Medium constraints have been accomplished by synthesized active sites [8,9]; functionalized porous solids [10,11] nanocages [3,4], zeolites or supramolecular aggregates [12,13].

The role of physical barriers imposed by structures, emphasizing a non bystander role, has been frequently evidenced by Rebek Jr or Fujita and collaborators among others, while exploring the entrapment of molecules within cages [3,5,14–18]. Likewise, other surface immobilization strategies, involving supported metal clusters, nanoparticles or metal complexes, have also been successfully accomplished [8–11]; in particular the interactions between metal complexes and surfaces, have been addressed by Yermakov and co-workers [9] as well as in our laboratory [19–21].

The catalyzed quaternization of silver (I) coordinated tertiary amines, in the presence of an insoluble silver salt, has been investigated in our laboratory. Other strategies to accelerate nitrogen quaternization, a very slow process, may be mentioned, namely the synthesis by means of resin bound tertiary amines [22], within deep cavitands [16] or even by the so-called "one pot reactions" involving amides as starting material [23].

The relevance of quaternary ammonium salts synthesis has been reinforced by the expanding range of applications, beyond the traditional uses as surfactants or phase transfer catalysts, in view of potential uses in battery technology, ionic liquids and drug development [4,23,24].

Our previous studies on the joint homogeneous–heterogeneous catalysis of triethylamine quaternization by alkyl halides [19–21] disclosed a complex process involving free and adsorbed coordinated triethylamine and alkyl halides. Herein coordinated silver nitrate acts as a structural promoter for the nucleophilic attack of the halide in solution and on the surface, due to a more favorable surface arrangement of the reacting amine and halide molecules. The extension of these studies to the silver promoted quaternization of tributylamine by alkyl iodides, apart from further testing the previously proposed model [20], enables a broader discussion of free and coordinated amine homogeneous–heterogeneous processes. Furthermore, the parallelism between solution and surface processes consents the establishment of a molecular level link between simultaneous homogeneous and heterogeneous process, occurring within a surface compartment of monolayer thickness.

* Corresponding author. Tel.: +351 21 7500896; fax: +351 21 7500088.
E-mail addresses: mssantos@fc.ul.pt (M. Soledade C.S. Santos), ester.barbosa@fc.ul.pt (E.F.G. Barbosa).

1381-1169/$ – see front matter © 2012 Elsevier B.V. All rights reserved.
doi:10.1016/j.molcata.2011.12.031

An approach which evidences how the specific surface imparted molecular confinement drives the heterogeneously catalyzed process.

2. Experimental

2.1. Reagents and solutions

The nominal purity of solvent, *Toluene* BDH *Aristar* grade, and reagents, *Tributylamine* BDH-GPR, *Ethyl iodide* BDH-GPR grade and *Butyl iodide* BDH-GPR grade, was checked by G.C., being 99.98% for the solvent *Toluene*, 94.47% for *Tributylamine*, 72.30% for *Ethyl iodide* and 99.75% for *Butyl iodide*. Accordingly, *Toluene* and *Butyl iodide* were used without further purification.

Ethyl iodide showed the yellowish color characteristic of photochemical decomposition [25]. Successive washings with dilute sodium thiosulfate solutions removed the free iodine. The final solution was dried with anhydrous calcium chloride, and finally fractionally distilled over sodium wire [25] leading to a distillate with 99.75% purity by G.C.

Tributylamine BDH-GPR, was treated with acetic anhydride and fractionally distilled, refluxed over potassium hydroxide and finally fractionally distilled from barium oxide through a column packed with Pyrex glass rings, under a reduced pressure of 1 kPa, as described by Barbosa and Lampreia [26], and showed a final purity of 99.98%.

Silver nitrate GPR grade (purity ≥ 99.8%) was supplied by BDH and was used without further purification. *Silver iodide* was synthesized before each run according to a procedure formerly described [19–21,27–29]. The polycrystalline solid obtained was predominantly composed of *β-AgI* and had a BET (N_2) specific surface area of $0.407 \pm 0.003\ m^2\ g^{-1}$ [29].

The amine, *ethyl* and *butyl iodide solutions* in toluene were prepared, by weight, in volumetric flasks and under a light N_2 flux as previously described [19–21].

2.2. Kinetic runs

The kinetic experiments were performed at $25.0 \pm 0.05\ ^\circ C$, under constant stirring, resorting to previously described procedures and experimental set up.

The kinetic runs were monitored collecting reaction mixture samples and determining by potentiometric back titration the amine and the silver content. This procedure ensured that the reaction under study was interrupted, in the collected sample mixtures, and simultaneously interferences in both analytical methods were avoided [19].

Amine titration: The amine concentration in sample reaction mixtures was determined by potentiometric back-titration, of an excess of perchloric acid (≈0.01 M) with standardized sodium hydroxide (≈0.04 M) because the acid–base titration, in anhydrous acetic acid, proved to be inappropriate due to the interference of silver ions [19].

Silver titration: The silver concentration in solution was determined by potentiometric back titration of an excess of standardized potassium iodide with silver nitrate in view of the difficulties associated with silver titration, in the presence of solids [19].

In Table 1 are summarized the initial conditions of the experimental kinetic runs used to obtain the relevant kinetic parameters for the reactions studied.

$$Bu_3N + Bu_3NAg^+NO_3^- + RI \xrightarrow{AgI} RBu_3N^+NO_{3\downarrow}^- + AgI_\downarrow + RBu_3N^+I_\downarrow^-$$

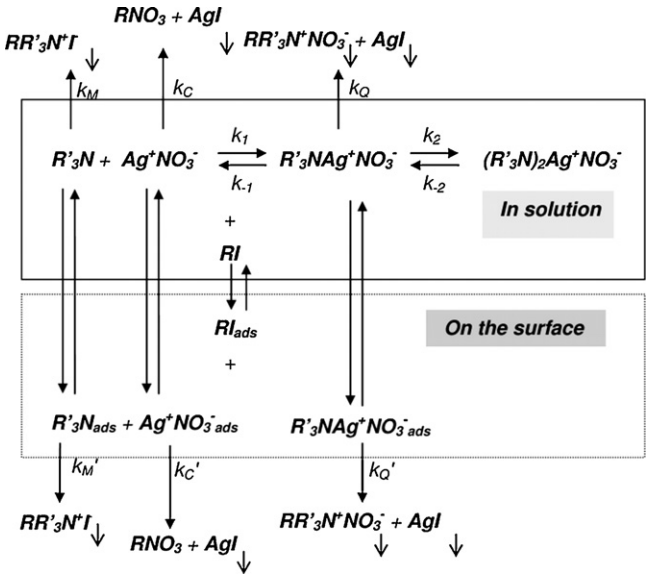

Scheme 1. Schematic representation of the molecular model proposed to interpret the silver iodide catalyzed quaternization of coordinated trialkylamines by alkyl iodides in toluene.

3. Results and discussion

3.1. Model framework

A brief description of the kinetic model used to analyze the kinetic data is outlined below, emphasizing exclusively the major landmarks for the sake of simplicity. The reaction Scheme 1, proposed earlier [19], to characterize the overall solution and surface process was considered once again. k_Q and k'_Q are the rate constants for the solution and surface catalyzed quaternization of the coordinated amine by the alkyl iodide, k_M and k'_M the solution and surface rate constants for the Menshutkin reaction, k_C the rate constant for the competitive solution reaction between silver nitrate and the ethyl iodide and $K_1 = k_1/k_{-1}$ and $K_2 = k_2/k_{-2}$ are the equilibrium constants for the formation of the 1:1 and 1:2 silver–amine complexes.

The total consumption of the reactants, alkyl iodide, trialkylamine and silver nitrate, includes solution and surface components, the overall rate equations were obtained neglecting the contribution of the terms referring to the Menshutkin reactions which are very slow ($10^{-6} \ll 10^{-3}\ M\ s^{-1}$), the alkylation reactions of the sterically hindered silver amine 1:2 complex, and the surface term of the reaction between free silver nitrate and alkyl iodide, that was disregarded versus its solution counterpart.

Accordingly

$$\frac{d[AgNO_3]_{total}}{dt} \cong \frac{d[RI]_{total}}{dt} > \frac{d[Et_3N]_{total}}{dt} \quad (1)$$

The corresponding differential rate expressions, containing solution and interfacial contributions were scrutinized in previous papers [20,21] and will not be repeated here. As before, integration of the complex differential equations was possible over extended periods of time, where the free amine concentration in solution remained almost constant [20,21], leading to

$$\ln\left(\frac{e - \phi x(t)}{a - x(t)}\right) = \ln\left(\frac{e - \phi x(t_{ac})}{a - x(t_{ac})}\right) - \left(k_Q + \frac{k_C}{K_1[Et_3N]_{free}}\right)(\phi a - e)Q_2(t - t_{ac}) \quad (2)$$

Table 1
Set of initial experimental conditions of the kinetic runs used to calculate the kinetic and adsorption parameters.

Initial conditions					
Run	Reagents	$[Bu_3NAgNO_3]$ (M)	[RI] (M)		m^0_{AgI} (g)
20[a]	$[Bu_3N]/M = 0.0391_1 [AgNO_3]/M = 0.0336_8$	0.0336_8	*EtI*	0.0413_5	0.00
21	$[Bu_3N]/M = 0.0391_9 [AgNO_3]/M = 0.0379_6$	0.0378_1	*EtI*	0.0399_0	0.7_5
22[a]	$[Bu_3N]/M = 0.0401_1 [AgNO_3]/M = 0.0340_4$	0.0336_5	*EtI*	0.0413_5	1.5_0
23[a]	$[Bu_3N]/M = 0.0387_2 [AgNO_3]/M = 0.0188_5$	0.0181_8	*EtI*	0.0400_7	0.00
24	$[Bu_3N]/M = 0.0393_8 [AgNO_3]/M = 0.0168_9$	0.0162_7	*EtI*	0.0400_7	1.5_2
25	$[Bu_3N]/M = 0.0380_3 [AgNO_3]/M = 0.0338_4$	0.0335_6	*EtI*	0.1570_8	0.00
26	$[Bu_3N]/M = 0.0380_3 [AgNO_3]/M = 0.0324_1$	0.0321_0	*EtI*	0.1570_8	1.5_6
27	$[Bu_3N]/M = 0.0385_7 [AgNO_3]/M = 0.0326_7$	0.0323_8	*BuI*	0.0394_4	0.00
28	$[Bu_3N]/M = 0.0403_2 [AgNO_3]/M = 0.0295_1$	0.0289_7	*BuI*	0.0392_6	0.7_4
29	$[Bu_3N]/M = 0.0393_8 [AgNO_3]/M = 0.0287_0$	0.0281_9	*BuI*	0.0391_1	1.5_8
30	$[Bu_3N]/M = 0.0388_4 [AgNO_3]/M = 0.0234_7$	0.0231_0	*BuI*	0.0391_1	0.00
31	$[Bu_3N]/M = 0.0393_8 [AgNO_3]/M = 0.0156_6$	0.0150_8	*BuI*	0.0391_1	1.5_4

[a] Experimental data set presented previously [19], and reanalyzed according to the model formerly extended [20].

with t_{ac} signaling the onset of the reaction period where the free amine concentration remains constant ($[Bu_3N] \cong \overline{[Bu_3N]} \pm 5\%$), a is the corresponding ($t = t_{ac}$) alkyl iodide concentration, $e = [Bu_3NAgNO_3]_{t_{ac}} - \phi[AgNO_3]t_{ac}$ and Q_2 includes the underlying dependencies on the catalyst mass and adsorption coefficients ($\varphi = b_{Bu_3N}/b_{RI}$).

$$Q_2 = k_Q + \frac{k_C}{K_1[\overline{Bu_3N}]_{free}} + \frac{k'_Q a_s m}{V} \cdot \frac{b_{Bu_3NAgNO_3} c_{mono_{Bu_3NAgNO_3}} c_{mono_{RI}}}{(1/b_{RI}) + [RI]_{t_{ac}} + \varphi[\overline{Bu_3N}]_{free}} \quad (3)$$

Likewise, the integrated rate equation for the overall amine consumption, valid within the same period, $t \geq t_{ac}$, is

$$\ln\left(\frac{c - \phi x_1(t)}{g - x_1(t)}\right) = \ln\left(\frac{c - \phi x_1(t_{ac})}{g - x_1(t_{ac})}\right) - k_Q(\phi g - c)Q_1(t - t_{ac}) \quad (4)$$

where c is the concentration of coordinated amine at t_{ac}, g is $[RI]_{t_{ac}} - [AgNO_3]_{t_{ac}}$ and Q_1, is a coefficient containing exclusively parameters dependent on the quaternization reaction namely k_Q, k'_Q and m

$$Q_2 = k_Q + \frac{k'_Q a_s m}{V} \cdot \frac{b_{Bu_3NAgNO_3} c_{mono_{Bu_3NAgNO_3}} c_{mono_{RI}}}{(1/b_{RI}) + [RI]_{t_{ac}} + \varphi[\overline{Bu_3N}]_{free}} \quad (5)$$

An identical reasoning, for experimental runs conducted under an excess of alkyl halide, leads to coefficients Q_3 and Q_4 which have been presented previously [20].

Plots of the left hand side of Eq. (2) and (4) versus $(t - t_{ac})$ show linear behavior, over extended time periods, with high correlation coefficients($r^2 > 0.99$), substantiating the model and allowing the determination of Q_n coefficients under various experimental conditions.

3.2. Evaluation of kinetic and adsorption parameters

Fig. 1 presents the plots obtained for runs 23 and 30 of the reaction between silver coordinated tributylamine with ethyl iodide and butyl iodide. The same behavior was observed for all other runs, substantiating the model.

The experimental coefficients Q_1 and Q_2, as well as the corresponding coefficients Q_3 and Q_4 obtained in the presence of an excess of alkyl halide [20], are presented in Table 2. All data was further analyzed in terms of subsets, obtained under identical experimental conditions. The application of the kinetic model enables the calculation of the rate constants for the solution quaternization (k_Q) and competitive reactions (k_C), as well as the estimate of surface term $k'_Q b_{Bu_3NAgNO_3}$ associated with the surface catalyzed quaternization (Table 3 and Figs. 2 and 3).

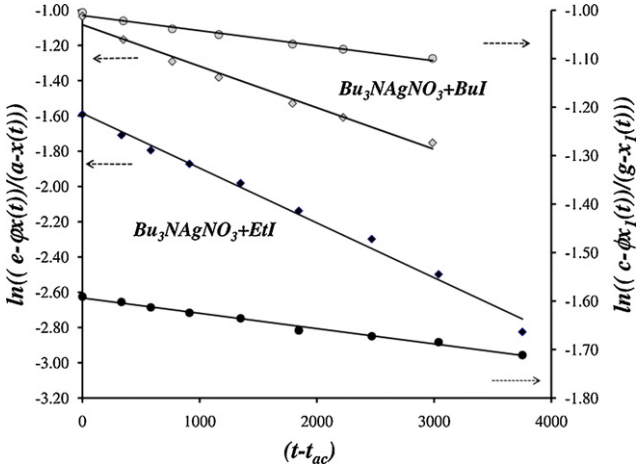

Fig. 1. Plots of Eqs. (2) and (4) for kinetic runs 23 and 30.

3.2.1. Side reaction between soluble silver nitrate and alkyl halides

Silver activated quaternization is accompanied by a competitive side reaction of the alkyl halide with free silver nitrate. Estimates of k_C for the reaction of free silver nitrate with ethyl iodide and butyl iodide in toluene were obtained independently, resorting to two different approaches. The first method consists in the use of expressions $k_C = K_1[\overline{Bu_3N}](Q_2 - Q_1)$ or $k_C = K_1[\overline{Bu_3N}](Q_4 - Q_3)$, obtained resorting to Eqs. (3) and (5). The second methodology involves extrapolation to zero mass of Q_2 and Q_1 or Q_4 and Q_3 where $Q_{1(m\to 0)} = Q_{3(m\to 0)} = k_Q$, thus $k_C = K_1[\overline{Bu_3N}](Q_{2n(m\to 0)} - Q_{2n-1(m\to 0)})$, see Eqs. (3) and (5) and Figs. 2 and 3.

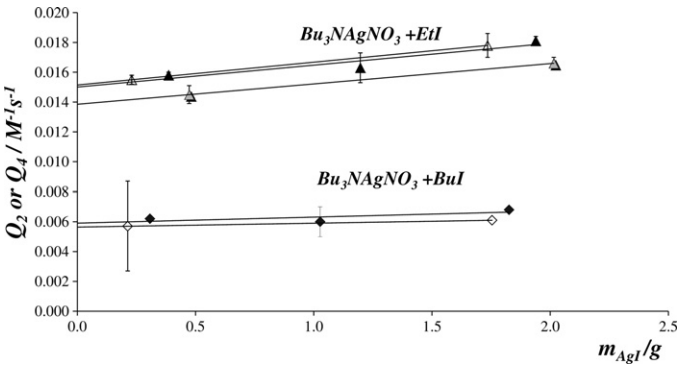

Fig. 2. . Dependence of Q_2 and Q_4 (runs 20–26 and 27–31) on the average mass of solid during the reaction period under study ($t \geq t_{ac}$).

Table 2
Calculated Q_1, Q_2, Q_3 and Q_4 coefficients as well as the corresponding free amine concentration for the reaction period under study ($t \geq t_{ac}$).

Run	t_{ac} (s)	$[\overline{Bu_3N}] \pm \sigma$ (M)	$[RI] \pm \sigma$ (M)	$Q_1 \pm \sigma$ ($M^{-1}\,s^{-1}$)	$Q_2 \pm \sigma$ ($M^{-1}\,s^{-1}$)	$Q_3 \pm \sigma$ ($M^{-1}\,s^{-1}$)	$Q_4 \pm \sigma$ ($M^{-1}\,s^{-1}$)
20	3373	0.028 ± 0.002	0.0165 ± 0.0003	0.00176 ± 0.00007	0.0158 ± 0.0002		
21	5032	0.024 ± 0.001	0.0145 ± 0.0003	0.00223 ± 0.00006	0.0163 ± 0.001		
22	1364	0.028 ± 0.001	0.0194 ± 0.0003	0.00244 ± 0.0001	0.0181 ± 0.0003		
23	841	0.032 ± 0.001	0.0270 ± 0.003	0.00158 ± 0.00008	0.0155 ± 0.0003		
24	1431	0.034 ± 0.001	0.0278 ± 0.0003	0.00211 ± 0.00006	0.0178 ± 0.0008		
25	1470	0.0317 ± 0.0008	0.1261 ± 0.0003			0.0014 ± 0.0003	0.0145 ± 0.0006
26	1348	0.033 ± 0.001	0.1281 ± 0.0003			0.0019 ± 0.0004	0.0166 ± 0.0004
27	5332	0.0241 ± 0.0009	0.0198 ± 0.0003	0.00059 ± 0.00004	0.0062 ± 0.0001		
28	2821	0.027 ± 0.001	0.0204 ± 0.0003	0.00071 ± 0.00006	0.006 ± 0.001		
29	1615	0.023 ± 0.001	0.0232 ± 0.0003	0.00092 ± 0.00003	0.0068 ± 0.0002		
30	1770	0.029 ± 0.0005	0.0242 ± 0.0003	0.00058 ± 0.00002	0.0057 ± 0.003		
31	1081	0.032 ± 0.002	0.0327 ± 0.0003	0.00089 ± 0.00004	0.0061 ± 0.0005		

The k_C values contained in Table 3 are all in agreement within the experimental error. Nonetheless a closer look at both approaches shows the latter one leads to more reliable estimates, an outcome expected in view of the multiple experimental runs required by this procedure. Hence, from this set of kinetic runs, the proposed values for k_c are $2.8 \pm 0.1 \times 10^3\ mol^{-1}\,dm^3\,s^{-1}$ and $1.02 \pm 0.07 \times 10^3\ mol^{-1}\,dm^3\,s^{-1}$ for the reactions of $AgNO_3 + EtI$, and $AgNO_3 + BuI$, in toluene, respectively.

3.2.2. Solution and surface catalyzed quaternization of silver (I) coordinated tributylamine by alkyl halides

Solution quaternization reaction rate constants, k_Q, for tributylamine with ethyl iodide and butyl iodide were determined by extrapolation to $m = 0$, Fig. 3, of coefficients Q_1 and Q_3, presented in Table 3. Best values, obtained by the weighted average of the extrapolated values are presented in Table 4, being $1.54 \pm 0.06 \times 10^{-3}\ mol^{-1}\,dm^3\,s^{-1}$ for $Bu_3N–AgNO_3 + EtI$ and $5.3 \pm 0.2 \times 10^{-4}\ mol^{-1}\,dm^3\,s^{-1}$ for $Bu_3N–AgNO_3 + BuI$.

The surface contribution to the quaternization reaction is evidenced by the mass dependent plots (Figs. 2 and 3) of Q_1, Q_2, Q_3 and Q_4, in accordance with Eqs. (3) and (5), where the dependency on the various adsorption quantities namely monolayer coverage, c_{mono}, and adsorption coefficients, b_i, for all species involved ($i = Et_3N$, RI and Et_3NAgNO_3) is explicit. For both amines adsorption coefficients and monolayer coverage were previously determined in our laboratory using the immersion technique. For the alkyl halides and the silver amine coordination compounds no data is available in the literature in this solvent; however as previously demonstrated [21], an adequate selection of experimental conditions provides indirect estimates of the halide adsorption coefficients magnitude (Eq. (6)). In the studies, involving Bu_3N and BuI, Eq. (6′), a general form of Eq. (6), was applied. The slope ratios of Q_n coefficients, namely Q_3/Q_1 or Q_1/Q_1, associated with various concentrations ($[RI]_{t_{ac}}$, $[\overline{Bu_3N}]$), allow an estimate of b_{RI} by iterative

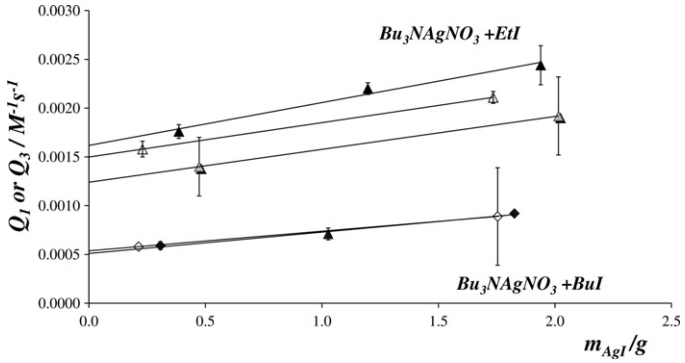

Fig. 3. Dependence of Q_1 and Q_3 (runs 20–26 and 27–31) on the average mass of solid during the reaction period under study ($t \geq t_{ac}$).

fit, as all other quantities involved in the ratio are known ($[RI]_{t_{ac}}$, $[\overline{Bu_3N}]$ and b_{Bu_3N}) or related ($\varphi = b_{Bu_3N}/b_{RI}$).

$$\frac{\theta_{EtI}/[EtI]_{t_{ac}}(\text{excess halide})}{1/((1/b_{EtI}) + [EtI]_{t_{ac}} + \varphi[\overline{Bu_3N}])} \cong \text{Constant} \quad (6)$$

$$\frac{(1/b_{BuI}) + [BuI]_{t_{ac}} + \varphi[\overline{Bu_3N}]}{1/((1/b_{BuI}) + [BuI]_{t_{ac}} + \varphi[\overline{Bu_3N}])} \cong \text{Constant}' \quad (6')$$

These independent evaluations result in $b_{EtI} = 19 \pm 4$ and $22 < b_{BuI} < 30$, confirming our previous educated guesses for both halides [21].

These estimates allow the calculation of "best values" for $k'_Q b_{Bu_3NAgNO_3}$ from the slopes of Eqs. (3) and (5), considering $a_s = 1.08\ m^2\,g^{-1}$, $c_{mono_{Bu_3N}} = 3.1 \times 10^{-6}\ mol\ m^{-2}$ [26] and $b_{EtI} = 19$ and $b_{BuI} = 22$, and lead to $1.6 \times 10^6\ m^2\,mol^{-1}\,s^{-1}$ and $6.7 \times 10^5\ m^2\,mol^{-1}\,s^{-1}$ for the surface quaternization with ethyl iodide and butyl iodide respectively, values which are included in Table 4.

4. Extended discussion of joint homogeneous and heterogeneous processes

The joint homogeneous–heterogeneous silver activated amine quaternization by alkyl halides is complex, involving various adsorption and solution equilibrium, as well as several kinetic steps on the surface and in solution. Having in mind a better understanding of the overall process, data obtained in this work was combined with previous studies on solution and surface quaternization of reactions $Et_3N–AgNO_3 + EtI$ and $Et_3N–AgNO_3 + BuI$ [19–21].

4.1. The side reaction between free silver nitrate and alkyl halides

The reaction between free silver nitrate and alkyl halides is always present while studying amine quaternization. The rate constants for the side reaction, determined here, for the tributylamine system, were $2.8 \pm 0.1 \times 10^3\ mol^{-1}\,dm^3\,s^{-1}$ for EtI and $10.2 \pm 0.7 \times 10^2\ mol^{-1}\,dm^3\,s^{-1}$ for BuI. Larger values have been reported earlier [21], for the same reactions, in the presence of triethylamine, $6.4 \pm 0.6 \times 10^3\ mol^{-1}\,dm^3\,s^{-1}$ and $5.5 \pm 0.2 \times 10^3\ mol^{-1}\,dm^3\,s^{-1}$.

The rate constants for the side reactions between silver nitrate and alkyl halides, determined in the presence of triethylamine are much larger than those reported here for the same reaction. These differences may be assigned to the unaccounted contributions of the corresponding surface catalyzed reactions, k'_C, in the mathematical development of the model. Nonetheless disregarding this contribution has no effect on the parameters [k_Q, k'_Q] for the quaternization reactions.

The most reliable estimates of k_C will correspond to a larger adsorption competition between free amine and

Table 3
Calculated k_C and k_Q for independent analysis of the experimental data sets.

Runs	$[\overline{Bu_3N}] \pm \sigma$ (M)	$k_C \pm \sigma$ ($M^{-1}\,s^{-1}$)		$k_Q \pm \sigma$ ($M^{-1}\,s^{-1}$)	$k'_Q\, b_{R_3NAgNO_3}$ ($m^2\,mol^{-1}\,s^{-1}$)
		$k_C = K_1[Bu_3N](Q_{2n} - Q_{2n-1})$	$k_C = K_1[Bu_3N](Q_{2n(m\to 0)} - k_Q) = K_1[Bu_3N](Q_{2n(m\to 0)} - Q_{2n-1(m\to 0)})$	$k_Q = Q_{2n-1(m\to 0)}$	$Q_n = k_Q + k'_Q m$
20	0.028 ± 0.002	0.386	$2.8 \times 10^3 \pm 3 \times 10^2$		
23	0.0317 ± 0.001	0.230	$3.2 \times 10^3 \pm 3 \times 10^2$		
25	0.0317 ± 0.0008	0.473	$2.9 \times 10^3 \pm 6 \times 10^2$		
20–22	0.0262 ± 0.0007	0.386–1.939		$1.61 \times 10^{-3} \pm 9 \times 10^{-5}$	1.68×10^6
23–24	0.0329 ± 0.0007	0.230–1.735	$2.5 \times 10^3 \pm 2 \times 10^2$	$1.51 \times 10^{-3} \pm 8 \times 10^{-5}$	1.60×10^6
25–26	0.0322 ± 0.0006	0.473–2.015	$3.2 \times 10^3 \pm 2 \times 10^2$	$1.3 \times 10^{-3} \pm 3 \times 10^{-4}$	1.64×10^6
27	0.0241 ± 0.0009	0.307	$2.9 \times 10^3 \pm 2 \times 10^2$		
30	0.029 ± 0.0005	0.213	$9.6 \times 10^2 \pm 1 \times 10^2$		
27, 29	0.0247 ± 0.0006	0.307–1.826	$1.1 \times 10^3 \pm 6 \times 10^2$	$5.23 \times 10^{-3} \pm 4 \times 10^{-5}$	6.3×10^5
28, 30, 31	0.030 ± 0.002	0.213–1.754	$1.0 \times 10^3 \pm 9 \times 10^1$	$5.27 \times 10^{-3} \pm 3 \times 10^{-5}$	7.1×10^5
			$1.1 \times 10^3 \pm 9 \times 10^1$		

alkyl halide, tributylamine rather than triethylamine data meet this condition. Consequently the best estimates for the solution rate constants of the side reactions *AgNO₃ + RI*, included in Table 4, are $2.8 \pm 0.1 \times 10^3$ $mol^{-1}\,dm^3\,s^{-1}$ for *EtI* and $10.2 \pm 0.7 \times 10^2$ $mol^{-1}\,dm^3\,s^{-1}$ for *BuI*.

Another interesting point is signaled while comparing the various rate constants for the side reactions. Larger decreases on k_C values, for the reactions with butyl iodide, indicate a bigger adsorption coefficient for this halide, a conclusion in agreement with the one obtained previously resorting to an independent approach [21].

4.2. Solution and surface catalyzed quaternization of silver (I) coordinated tertiary amines by alkyl halides

Values previously obtained for the solution and surface quaternization reactions *Et₃N–AgNO₃ + EtI* and *Et₃N–AgNO₃ + BuI* [20,21] were also included in Table 4 to allow a full comparison. These results show silver coordination significantly lowers the activation energy for solution amine quaternization, resulting in rate constants increases of 10^3 times. Moreover in the presence of solubilized silver nitrate a reduction of 2.2 in the rate constants, for tertiary amine quaternization by *EtI* [19], on going from triethylamine to tributylamine, is observed against a 5.3 times reduction in the absence of silver indicating a significant decrease on the transition state stereochemical constraints (Tables 4 and 5). The role of silver as a carbon—halogen bond cleavage activator is also evidenced by the smaller decrease on rate constants ratios (from 5.8 to 2.8) for the reaction of *Et₃N + RI*, on going from *EtI* to *BuI*, in the presence of silver nitrate (Table 4).

An overall analysis of the solution quaternization reactions in the presence of solubilized silver nitrate evidences a slightly larger decrease in the quaternization rate constants, associated with a two carbon increase in the halide chain length (2.8–2.9), than with the same chain length increase on the tertiary amine (2.2–2.4). Data indicating that, in the homogeneous pathway, the role of solubilized silver nitrate is more significant in terms of minimizing transition state stereochemical constraints than as a carbon halogen bond electrophilic activator.

In terms of the surface reaction, silver–amine coordination is crucial for the amine attack on a next neighbor halide. In fact quaternization by uncoordinated amine leads to inhibition in the presence of solids [30], while silver coordination accomplishes the lifting of the amine lone electron pair one atomic layer away from the surface, rendering adequate stereochemical positioning for the surface reaction.

As before, a thorough study of the surface catalyzed quaternization reactions analysis can be made resorting to herein reported and previously published data [20,21]. The values for $k'_Q\, b_{Et_3NAgNO_3}$ were recalculated, in order to optimize comparisons between different experimental data sets. The same adsorption coefficients for the alkyl halides, namely $b_{EtI} = 19$ and $b_{BuI} = 22$, were considered and the final values compiled in Table 4

The decrease in the experimental ratios associated with an increase of the alkyl halide chain length are larger for the quaternization of coordinated triethylamine (3.2) than for coordinated tributylamine (2.5) indicating smaller stereochemical constraints on the latter amine (Table 4). This apparently inconsistent result is in accordance with previously predicted minor deviations from spherical towards barrel type geometry for adsorbed tributylamine [29].

The relationships between reactions of the same alkyl halide with either amine are not straightforward as the ratios $k'_Q b_{Et_3NAgNO_3} / k'_Q b_{Bu_3NAgNO_3}$ entail products of surface reactions rates by adsorption coefficients. Surface rate constants, k'_Q, could not be explicitly obtained, due to the unavailability of adsorption

Table 4
Rate constants for all reactions associated with amine quaternization in the presence and absence of solubilized silver nitrate and consequences of halide alkyl chain length increase on all processes.

	$R_3N + RI$		$R_3N–AgNO_3 + RI$					
	k_M ($M^{-1}\,s^{-1}$)	$\frac{k_{M(EtI)}}{k_{M(BuI)}}$	k_C ($M^{-1}\,s^{-1}$)	k_Q ($M^{-1}\,s^{-1}$)	$k'_Q b_{R_3NAgNO_3}$ ($m^2\,mol^{-1}\,s^{-1}$)	$\frac{k_{C(EtI)}}{k_{C(BuI)}}$	$\frac{k_{Q(EtI)}}{k_{Q(BuI)}}$	$\frac{k'_{Q(EtI)}}{k'_{Q(BuI)}}$
$Et_3N + EtI$	3.3×10^{-6}	5.8	$6.4 \times 10^{3} \pm 6 \times 10^{2}$	$3.46 \times 10^{-3} \pm 2 \times 10^{-4}$	5.0×10^{6}	1.2 ± 0.2	2.8 ± 0.2	3.2
$Et_3N + BuI$	5.6×10^{-7}		$5.5 \times 10^{3} \pm 2 \times 10^{2}$	$1.244 \times 10^{-3} \pm 2 \times 10^{-6}$	1.5×10^{6}			
$Bu_3N + EtI$	6.2×10^{-7}	–	$2.8 \times 10^{3} \pm 1 \times 10^{2}$	$1.54 \times 10^{-3} \pm 6 \times 10^{-5}$	1.6×10^{6}	2.8 ± 0.3	2.9 ± 0.3	2.5
$Bu_3N + BuI$	–		$1.0 \times 10^{3} \pm 7 \times 10^{1}$	$5.3 \times 10^{-4} \pm 2 \times 10^{-5}$	6.7×10^{5}			

Table 5
Effect of trialkylamine chain length on the rate constants for all reactions associated with amine quaternization in the presence of solubilized silver nitrate, and comparative analysis of the results obtained by the strategies used to estimate $b_{Et_3NAgNO_3}/b_{Bu_3NAgNO_3}$.

R_3N-$AgNO_3$+RI	$\frac{k_C(Et_3N)}{k_C(Bu_3N)}$	$\frac{k_Q(Et_3N)}{k_Q(Bu_3N)}$	$\frac{k'_Q b_{Et_3NAgNO_3}}{k'_Q b_{Bu_3NAgNO_3}}$	$\frac{k'_Q b_{R_3NAgNO_3}}{k_Q}$ /10^3 m^{-1}	$\frac{b_{Et_3NAgNO_3}}{b_{Bu_3NAgNO_3}}$	$\frac{k'_Q\ Et_3N}{k'_Q\ (Bu_3N)}$	h_{mono} /m	$\frac{k'_Q b_{R_3NAgNO_3} h_{mono}}{k_Q}$	$\frac{b_{Et_3NAgNO_3}}{b_{Bu_3NAgNO_3}}$
Et_3NAgNO_3+EtI	2.3±0.3	2.2±0.2	3.1	1.43×10^{9} [a]	1.31	2.3	9.54×10^{-10}	1.4×10^{3} [b]	1.24
Bu_3NAgNO_3+EtI				1.09×10^{9} [a]			1.10×10^{-9}	1.2×10^{3} [b]	
Et_3NAgNO_3+BuI	5.4±0.8	2.4±0.1	2.3	1.43×10^{9} [a]		1.8	1.11×10^{-9}	1.4×10^{3} [b]	
Bu_3NAgNO_3+BuI				1.09×10^{9} [a]			1.11×10^{-9}	1.2×10^{3} [b]	

[a] See Fig. 4.
[b] See Fig. 5.

coefficients for silver–amine complexes, $b_{R_3NAgNO_3}$. Nevertheless the ratio $b_{Et_3NAgNO_3}/b_{Bu_3NAgNO_3}$, can be indirectly attained following two different approaches:

(i) Plots of $k'_Q b_{R_3NAgNO_3}$ versus k_Q were drawn for experiments of the same amine and variable alkyl halide (Fig. 4), and the zero intercepts allowed the calculation of 1.31 for the ratio of the silver–amine complexes adsorption coefficients.
(ii) Another independent reasoning, focused on the silver coordination sphere, was also pursued. Within this framework the parallelism between the exchange of an electron donating solvent molecule by a second amine molecule in solution, and the adsorption of the coordinated amine, involving the substitution of a solvent molecule by a surface iodide, was examined. This assumption means the ratio $b_{Et_3NAgNO_3}/b_{Bu_3NAgNO_3}$ may be approximated by the quotient of the second stepwise formation constants for the corresponding silver–amine complexes in solution $K_{2(Et_3N)}/K_{2(Bu_3N)} = 1.59$ [31].

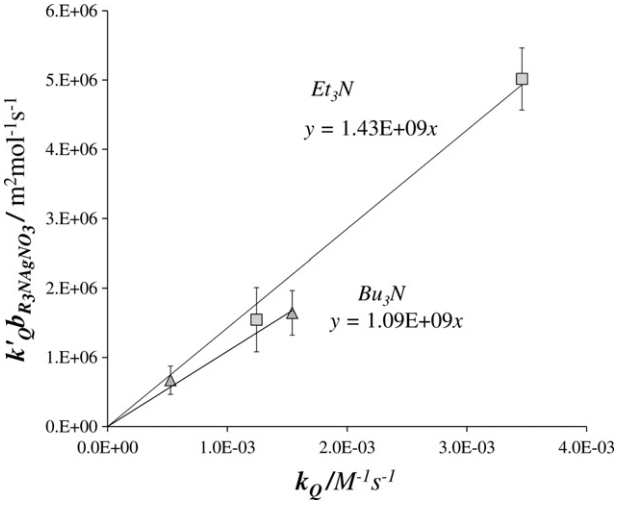

Fig. 4. Dependence of $k'_Q b_{R_3NAgNO_3}$ on k_Q for the quaternization of coordinated trialkylamines.

The higher basicity of triethylamine in toluene [29,31] is a premise setting 1.59 as an upper limit for the corresponding ratio of adsorption coefficients, a hypothesis in conformity with the preceding guesstimate, 1.31, which will be used from here on in this discussion. Once a reliable estimate for the ratio of the silver amine complexes adsorption coefficients is obtained, one may calculate the ratio of the surface reaction rates involving the same halide and different amines. Taking 1.31 as a trustworthy ratio 2.3 is obtained for the ratio of the quaternization reactions of silver coordinated amines ($k'_Q b_{Et_3NAgNO_3}/k'_Q b_{Bu_3NAgNO_3}$) with ethyl iodide and 1.8 for the corresponding reactions with butyl iodide, values which were included in Table 5.

A comparison between the ratios of solution and surface reactions evidences that surface packing constraints are efficiently reduced (2.2–2.3) or even surpassed (2.4–1.8) by the concomitant carbon—halogen bond activation of silver ions, either solubilized or on the solid surface.

These results demonstrate the decrease on the surface quaternization reaction rates, with increasing chain length, is less accentuated for changes in alkyl halide chain length thus evidencing that apart from the usefulness of silver coordination in terms of amine positioning, silver activation of the carbon–halide bond stands as the driving force in the surface catalyzed pathway. This reinforced electrophilic effect on surface pathways has its costs in terms of the parallel reaction, which is noteworthy for the longer alkyl halides, and entails a reduction of overall quaternization reaction yield.

The pursuit of a broader understanding of these homogeneous–heterogeneous systems led to a molecular level inspection of the surface monolayer where the surface reaction occurs. The surface monolayer thickness, h_{mono}, is determined by the nature, size and molecular geometry of the adsorbed entities involved in the reaction. The thickness of a monolayer

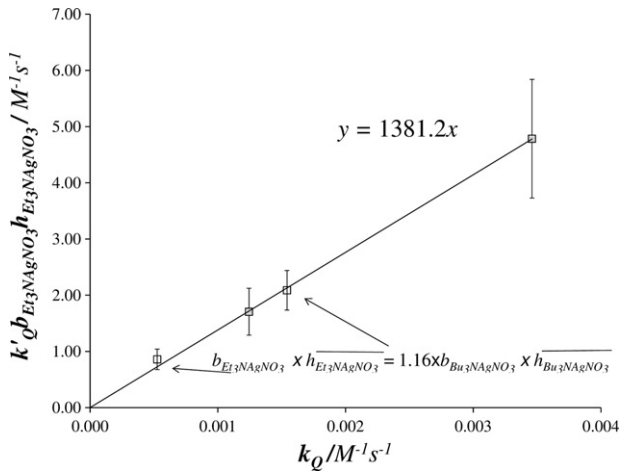

Fig. 5. Relation between $k'_Q b_{Et_3NAgNO_3} h_{mono}$ and k_Q for the quaternization of coordinated trialkylamines considering $b_{Et_3NAgNO_3} h_{Et_3NAgNO_3} / b_{Bu_3NAgNO_3} h_{Bu_3NAgNO_3} = 1.16$.

of adsorbed alkyl halide was approximated by the length of a linear hydrocarbon $l_{CH_3(CH_2)_n} \cong 1.57 + 1.27\,n$ Å plus a covalent iodide diameter [32,33] rendering $h_{monoEtI} = 8.51 \times 10^{-10}$ m and $h_{monoBuI} = 1.11 \times 10^{-9}$ m. For coordinated amines, adsorbed on *AgI*, monolayer thicknesses were calculated resorting to silver ionic diameter [32] and to the adsorbed tertiary amine diameters, obtained from experimental molar volumes and considering a hexagonal close-packed arrangement of molecules over a bidimensional surface [29,32], leading to monolayer thicknesses of $h_{monoEt_3NAgNO_3} = 9.54 \times 10^{-10}$ m and $h_{monoBu_3NAgNO_3} = 1.10 \times 10^{-9}$ m.

These quantities consent the transformation of surface rate constants, k'_Q, into "volumetric surface rate constants" (a new designation, found appropriate for this quantity) for the reaction within a tridimensional space on the surface, enabling a clear cut identification of the surface role.

Plots of $k'_Q b_{R_3NAgNO_3} h_{mono}$ versus k_Q, presented in Fig. 4, display different slopes, dependent on the adsorption coefficients of the tertiary amine silver complexes, $b_{R_3NAgNO_3}$. All the data may be drawn to a common line (Fig. 5) upon the introduction of the constant factor 1.16, thus enabling the calculation of 1.24 for the ratio between adsorption coefficients, a value providing additional validation for 1.31 previously proposed in (i).

The slope of the superimposed linear plots, presented in Fig. 5, evidences clearly the catalytic effect of the *AgI* surface on the silver coordinated quaternization of tertiary amines reaction. However the precise value for the "volumetric surface rate constants" cannot be determined as values for $b_{R_3NAgNO_3}$ are not available. Nevertheless, bearing in mind amine electron donation will lead to a reduction in the adsorption coefficient reported for silver nitrate in water [34], and also considering the magnitude estimated here for alkyl halides adsorption coefficients, a broad boundary may be set, consenting the proposal of a tenth magnitude for the silver amine complex adsorption coefficient on silver iodide in toluene. Accordingly one may conclude that "volumetric surface rate constants" are 10^2 times higher than the corresponding solution rate constants.

This rate increase was observed with *AgI*, an extremely low surface area solid ($1.08\ m^2\ g^{-1}$ [29]), chosen to ensure the presence of Ag^+ and I^- surface sites, and warranting an identity between parallel solution and surface processes, thus enabling the comparison between the two reaction pathways. In view of the results, obtained for this model system, much larger rate enhancements are foreseen for higher surface area solids.

5. Conclusions

This is the last of a series of studies for a homo/heterogeneous processes, developed in our laboratory, on the quaternization of tertiary amines by alkyl iodides in toluene. In particular, the role of added silver ions in solution and solid *AgI* was investigated for this model system.

The new data presented here confirm that the multiple step model, built in preceding work, its mathematical description and development, with a careful analysis of errors, generates consistent and coherent results. The combination of different parameters, obtained for all systems explored, establishes silver ions act as structural promoter, minimizing stereochemical constraints, and as carbon halogen bond cleavage activators. These conclusions are consistent with a balance dominated by structural factors in the solution process which are reinforced and exceeded by electronic effects in the surface pathway.

The perfect parallelism between homogeneous and heterogeneous silver (I) activated quaternization of tertiary amines by alkyl iodides, in this model system, supported a molecular level analysis of the heterogeneous process. This strategy allowed the identification of a surface compartment of monolayer thickness, h_{mono}, determined by size, shape and orientation of the chemical species on the surface. "Volumetric surface rate constants" were estimated and directly compared with their solution counterparts, providing a clear-cut link between the homogeneous and heterogeneous processes. Finally, it is believed this model system and molecular analysis is a contribution for future approaches of complex homo/heterogeneous systems.

Acknowledgments

This work was funded by National Funds (PEst-OE/QUI/UI0612/2011) through FCT – Fundação para a Ciência e a Tecnologia.

References

[1] K.I. Zamaraev, in: J.M. Thomas, K.I. Zamaraev (Eds.), Perspectives in Catalysis, Blackwell Scientific Publications, London, 1992, pp. 35–37.
[2] G.A. Somorjai, M.C. Yang, Top. Catal. 24 (2003) 61–72.
[3] M. Yoshizawa, Y. Takeyama, T. Okano, M. Fujita, J. Am. Chem. Soc. 125 (2003) 3243–3247.
[4] J.J. Davis, Chem. Commun. 28 (2005) 3509–3513.
[5] M.P. Schramm, R.J. Hooley, J. Rebek Jr, J. Am. Chem. Soc. 129 (2007) 9773–9779.
[6] G.A. Somorjai, J.Y. Park, Angew. Chem. Int. Ed. 47 (2008) 9212–9228.
[7] G.A. Somorjai,.H. Frei, J.Y. Park, J. Am. Chem. Soc. 131 (2009) 16589–16605.
[8] A. Vazquez-Zavala, J. Garcia-Gomez, A. Gomez-Cortes, Appl. Surf. Sci. 167 (2000) 177–183.
[9] B.L. Moroz, V.A. Semikolenov, V.A. Likholobov, Y.I. Yermakov, J. Chem. Soc. Chem. Commun. (1982) 1286–1287.
[10] K.H. Park, S. Uk Son, Y.K. Chung, Chem. Commun. (2003) 1898–1899.
[11] J. Guzman, B.C. Gates, Dalton Trans. (2003) 3303–3318.
[12] V. Ramamurthy, J. Shailaja, L.S. Kaanumalle, R.B. Sunoj, J. Chandrasekhar, Chem. Commun. (2003) 1987–1999.
[13] M.S. Masar, N.C. Gianneschi, C.G. Oliveri, C.L. Stern, S.T. Nguyen, C.A. Mirkin, J. Am. Chem. Soc. 129 (2007) 10149–10158.
[14] R.J. Hooley, J. Rebek Jr., J. Am. Chem. Soc. 127 (2005) 11904–11905.
[15] B.W. Purse, J. Rebek, Proc. Natl. Acad. Sci. U. S. A. 102 (2005) 10777–10782.
[16] B.W. Purse, A. Gissot, J. Rebeck Jr., J. Am. Chem. Soc. 127 (2005) 11222–11223.
[17] R.J. Hooley, H. Van Anda,.J. Rebek Jr., J. Am. Chem. Soc. 129 (2007) 13464–13473.
[18] K. Nakabayashi, M. Kawano, M. Yoshizawa, S. Ohkoshi, M. Fujita, J. Am. Chem. Soc. 126 (2004) 16694–16695.
[19] M. Soledade C.S. Santos, Ester F.G. Barbosa, J. Mol. Catal. A: Chem. 160 (2000) 293–313.
[20] M. Soledade C.S. Santos, Ester F.G. Barbosa, J. Mol. Catal. A: Chem. 197 (2003) 73–90.
[21] M. Soledade C.S. Santos, Ester F.G. Barbosa, J. Mol. Catal. A: Chem. 306 (2009) 82–88.
[22] K.S. Cameron, J.R. Morphy, Z. Rankovic, M. York, J. Comb. Chem. 4 (2002) 199–203.
[23] J. Ropponen, M. Lahtinen, S. Busi, M. Nissinen, E. Kolehamainen, K. Rissanen, New J. Chem. 28 (2004) 1426–1430.
[24] V. Calo, A. Nacci, A. Monopoli, A. Fanizzi, Org. Lett. 4 (2002) 2561–2563.

[25] D.D. Perrin, W.L.F. Armarego, D.R. Perrin, Purification of Laboratory Chemicals, 2nd Ed., Pergamon Press, Oxford, 1982, pp. 165.
[26] E.F.G. Barbosa, I.M.S. Lampreia, Can. J. Chem. 64 (1986) 387–393.
[27] H.J. van den Hul, J. Lyklema, J. Am. Chem. Soc. 90 (1968) 3010–3015.
[28] E.W. Sidebottom, W.A. House, M.J. Jaycock, J. Chem. Soc. Faraday Trans. 72 (1976) 2709–2721.
[29] M.S.C.S. Santos, E.F.G. Barbosa, J. Phys. Chem. B 102 (1998) 6040–6048.
[30] E.F.G. Barbosa, M. Spiro, J. Chem. Soc. Chem. Commun. (1977) 423–424.
[31] M. Soledade C.S. Santos, E.F.G. Barbosa, M. Spiro, J. Chem. Soc. Faraday Trans. 84 (1988) 4439–4449.
[32] R.D. Shannon, Acta Crystallogr. A32 (1976) 751–767.
[33] A.Y. Meyer, D. Farin, D. Avnir, J. Am. Chem. Soc. 108 (1986) 7897–7905.
[34] J. Austin, O. Ibrahim, M. Spiro, J. Chem. Soc. 6 (1969) 669–674.